INSTITUTE OF PHYSICS PUBLISHING JOURNAL OF PHYSICS: CONDENSED MATTER

J. Phys.: Condens. Matter **17** (2005) 2269–2279 doi:10.1088/0953-8984/17/15/002

Liquid–liquid phase transition in Stillinger–Weber silicon

Philippe Beaucage and Normand Mousseau

Département de Physique and Regroupement Québécois sur les Matériaux de Pointe, Université de Montréal, CP 6128, Succursale Centre-ville, Montréal, QC, H3C 3J7, Canada

E-mail: Normand.Mousseau@umontreal.ca

Received 9 December 2004, in final form 18 February 2005
Published 1 April 2005
Online at stacks.iop.org/JPhysCM/17/2269

Abstract

It was recently demonstrated that Stillinger–Weber silicon undergoes a liquid–liquid first-order phase transition deep into the supercooled region (Sastry and Angell 2003 *Nat. Mater.* **2** 739). Here we study the effects of perturbations on this phase transition. We show that the order of the liquid–liquid transition changes with negative pressure. We also find that the liquid–liquid transition disappears when the three-body term of the potential is strengthened by as little as 5%. This implies that the details of the potential could affect strongly the nature and even the existence of the liquid–liquid phase.

1. Introduction

The amorphous phase of Si is particular in that it does not correspond to the arrested liquid phase, contrarily to glasses: while liquid Si is metallic, with an average coordination around 6.4 at ambient conditions [41, 42, 20], a-Si has a coordination near 4 and is a semiconductor. The existence of a possible intermediate phase, explaining in part this difference, was first suggested by Aptekar, who showed that the Gibbs free energy of the amorphous phase does not extrapolate smoothly to that of the liquid, indicating that an additional phase transition should occur at around 1450 K [9]. Much experimental [8, 18, 39, 11] and numerical work [4, 7, 29, 28] followed, supporting the existence of such an additional phase, long thought to be the amorphous phase.

A breakthrough in the understanding of this unusual feature came a few years ago with the first clear experimental evidence for liquid polymorphism in a number of materials such as Y_2O_2–Al_2O_3 [1]. The distinct liquid phase hypothesis was first formulated to explain several properties of water near the melting temperature, including the density anomalies, and was supported by the polymorphism of the crystal and amorphous phases. More precisely, Mishima *et al* [30, 31] proposed that the liquid–liquid transition for water between a low density liquid

(LDL) and a high density liquid (HDL) is the continuity at higher temperatures of the known amorphous phase transition between the low and high density forms.

In analogy with water, it was rapidly suggested that a 'fragile-to-strong' liquid transition occurs in the supercooled regime of silicon, the resulting viscous liquid at low temperature (i.e. LDL) corresponding to the precursor phase of the amorphous metastable state [5–7]; the best candidates for showing such a liquid–liquid phase transition are tetravalent systems, which display an open molecular structure, such as H_2O, C, Si, Ge, SiO_2 and GeO_2 which all show a density maximum as a function of temperature [34, 37, 35]. *Ab initio* numerical calculations [19] also show a transition between a low (LDA) and high (HDA) density amorphous phase of silicon under high pressure, providing additional support for this hypothesis. More importantly, the liquid–liquid transition for silicon is not excluded from the stable region of the phase diagram and recent experimental work on liquids revealed a structural change for liquid Si [22], GeO_2 [33] and P [25] under high pressure.

Recently, the first clear demonstration of the existence of this low density liquid phase, at least for the Stillinger–Weber silicon, was given by Sastry and Angell [36]. They identify a first-order liquid–liquid phase transition taking place around 1060 K by measuring the heat release in a simulation in the *NPH* ensemble, finding results in agreement with a number of previous simulations. They showed, moreover, that the resulting phase is a very viscous tetrahedral liquid which should be the precursor to the well-characterized amorphous phase.

Although this pioneering work establishes the existence of the liquid–liquid phase transition, it is essential to characterize the behaviour of this transition under perturbations. In this paper, we study the impact of pressure and potential modifications on this transition. In particular, we find that the amorphous phase does correspond to the low density liquid at zero pressure. However, we also find that the liquid–liquid transition changes order with negative pressure. We show that this transition becomes unreachable with a very slight change of the SW potential, indicating that while this transition is clearly present for this potential, it remains to be fully demonstrated for real Si.

2. Methods

The molecular dynamical simulations for this work are performed in three ensembles: isobaric (*NPE*), isothermal–isobaric (*NPT*) and iso-enthalpic–isobaric (*NPH*). All simulations are done at $P = 0$ in a cubic box containing 1000 atoms, with periodic boundary conditions. The extended-system method of Andersen is used to control pressure [3, 23, 16] and Hoover's constraint method for the temperature [24, 21, 2]. We use the fifth-order Gear predictor–corrector to integrate Newton's equation with a time step $\Delta t = 1.15$ fs. Typically, after a change in temperature, the simulations are equilibrated for 50 000 Δt (58 ps) and statistics are accumulated over 450 000 Δt (518 ps).

Atomic interactions are represented by the Stillinger–Weber (SW) potential, developed to reproduce accurately the crystalline and the liquid state of Si [38]. Although this potential has known limitations, especially in the amorphous phase [28, 29, 13, 40], it ensures a reasonable description of the liquid phase [17, 12, 15]. Its melting temperature is also near the experimental value of 1683 K [10]: averaging the temperature of a box with a crystal–liquid interface at equilibrium, we find a temperature of 1662 ± 1 K, in agreement with $T_m = 1665$ K found by Landman *et al* [27] using a similar method.

To measure directly the degree of local crystallinity in the liquid and amorphous phases, we use a set of criteria that identify the smallest three-dimensional structures associated with wurtzite, diamond and β-tin crystalline structures (see figure 1). We restrict this topological analysis to pairs of atoms that are within 2.75 Å of each other to ensure that these atoms are close to a crystalline or amorphous environment. For all other quantities, we consider the first-

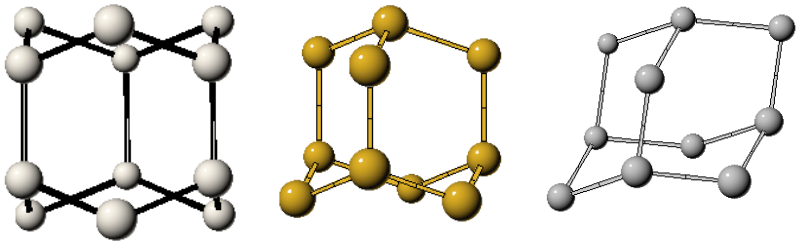

Figure 1. The three basic building blocks which represent the order parameter for characterizing the state of crystallization of the model. The wurtzite basic block (left) is a 12-atom cluster composed of two sixfold rings whereas the diamond basic block (centre) is a 10-atom cluster with four sixfold rings. The β-tin basic block (right) is equal to a diamond basic block where the tetrahedra are compressed in one direction and elongated along the two other axes.

(This figure is in colour only in the electronic version)

neighbour cut-off to be at the first minimum between the first- and second-neighbour peaks in the radial distribution function (RDF). The connection between neighbours must form closed loops according to the diamond and wurtzite structures but regardless of the bonds orientation. The wurtzite elementary block is a 12-atom cluster with two sixfold rings stacked on top of each other and connected by three bonds; the elementary building block for both diamond and β-tin has the same topology consisting of four six-membered rings placed back to back, forming a ten-atom cluster. These elementary clusters are only present with a low density in good quality amorphous Si relaxed with the SW potential (10–20 at.%) as well as in the HDL (5–10 at.%) providing a very convenient measure of local crystalline order; they were used for the same purpose in a previous study of crystallization [32]. This order parameter is a much more sensitive measure of crystallinity than the structure factor or the RDF.

3. Results

3.1. Liquid–liquid transition

3.1.1. Zero pressure. The Stillinger–Weber liquid-to-amorphous transition was one of the first problems studied after the potential was introduced. Broughton and Li observed that supercooled silicon transforms continuously into a glass at low temperature [15]. Further investigations by Luedtke and Landman, however, showed that the liquid undergoes a first-order phase transition at around 1060 K, transforming directly into a reasonably good quality amorphous solid if the simulated cooling down is slow enough [28, 29]. This phase was found to be reversible as the system is heated from the amorphous phase. Following recent work on polymorphism in liquids, Angell and Borick [4] suggested that the phase just below the transition temperature is not an amorphous solid but a very viscous liquid, freezing into the amorphous phase. As discussed in the introduction, this suggestion was recently demonstrated by Sastry and Angell using an elegant analysis [36]: simulating undercooling of l-Si in the *NPH* ensemble, it is possible to show unequivocally that the system undergoes a first-order liquid–liquid transition from a high density liquid (HDL) to a low density liquid (LDL) before transforming continuously to the amorphous state, a thermodynamically metastable state.

Our simulations find the same first-order liquid–liquid phase transition near 1060 K as the system is cooled slowly from high temperature. Figure 2 shows the density as a function of the temperature in the *NPT* ensemble with steps of -30 and -5 K between points while the *NPH* data are obtained in steps of -5 K. Small temperature steps are needed to see the details

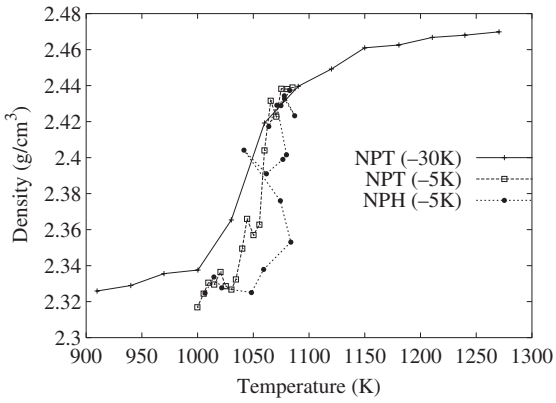

Figure 2. Mean density as a function of temperature for a 1000-atom SW cell at zero pressure. Simulations start with a well-equilibrated model of l-Si at 1300 and 1090 K for temperature steps of -30 and -5 K respectively. The first two simulations are performed in the *NPT* ensemble, with the temperature lowered in steps of 30 K (crosses and solid curve) and 5 K (open squares and dashed curve) while the last curve shows the density as a function of temperature for simulations in the *NPH* ensemble in which the temperature is decreased by steps of 5 K (filled circles and dashed curve, open circles and dotted curve). Curves are guides to the eye.

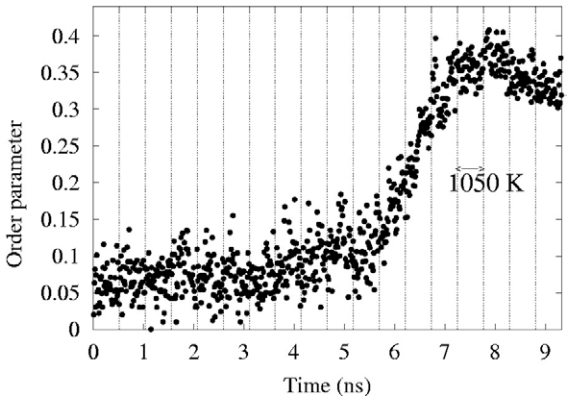

Figure 3. Evolution of the proportion of atoms in crystalline structures for the simulation in the *NPH* ensemble at zero pressure. Each section represents a time interval at a given enthalpy with the kinetic energy reduced by 5 K at the end of each interval. Each interval correspond to a thermodynamic point in the density versus temperature figure (see figure 2). The double arrow indicates the time interval for which the average temperature is 1050 K.

of the first-order liquid–liquid transition. Each of these points is obtained by averaging over 450 000 time steps, after a 50 000 time step equilibration period. As explained in [36], the discontinuities in the *NPH* curve are associated with a first-order transition. The transition is also clearly visible in the density: the system expands abruptly as it is cooled from 1090 to 1050 K and its density falls from 2.44 to 2.32 g cm^{-3}. This change in volume is associated with a lowering of coordination from 4.9 to 4.24 as the system becomes more like a network liquid.

The LDL possesses a largely tetrahedral structure with a coordination of 4.24 at 1050 K in the *NPH* ensemble, near the 4.2 value reported by Sastry and Angell [36]. The topological analysis, using the elementary blocks, shows that 37% of the atoms are associated with a basic building block; the structure is partially crystallized (figure 3) whereas the HDL phase

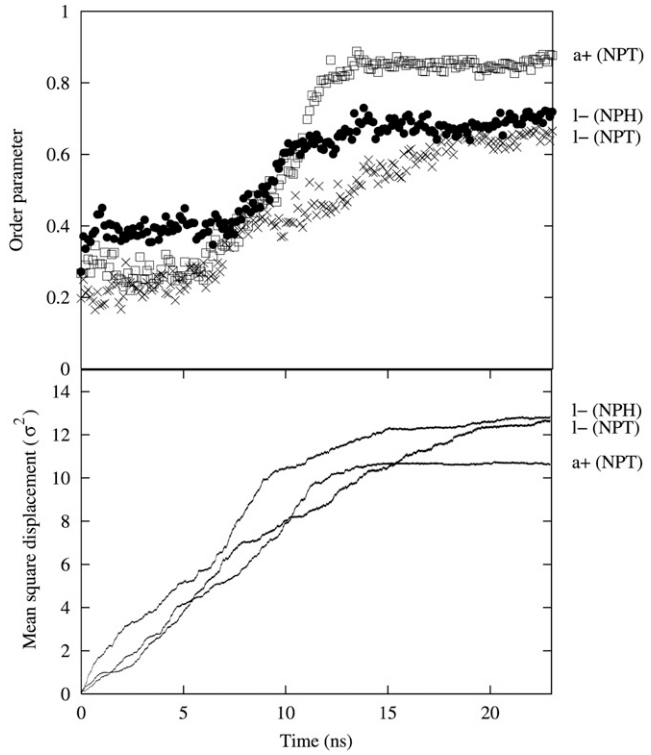

Figure 4. The proportion of atoms belonging to basic building-block structures (top) and the mean square displacements per atom (bottom) for simulation performed at a constant temperature ($T = 1050$ K). The initial liquid configurations at 1050 K are obtained from the cooling simulations in the *NPT* 'l-(*NPT*)' and *NPH* 'l-(*NPH*)' ensembles and are run in the same ensemble. The initial amorphous model was obtained by heating to 1050 K in the *NPT* ensemble 'a+(*NPT*)'.

at $T = 1090$ K contains only 5–10 at.% of elementary blocks. While the LDL contains a large fraction of elementary blocks, it remains homogeneous: on average each atom is part of a crystalline structure 25% of the time, with every atom belonging to a crystallite at least once. Since the LDL phase transforms continuously to the amorphous state as temperature decreases, the number of crystalline blocks should also decline to recover the low value of the amorphous phase and we do observe this tendency from figure 3. The diffusion of atoms changes abruptly during the transition and the diffusivity of the quenched liquids at 1050 K is 3.2×10^{-8} and 3.8×10^{-7} cm^2 s^{-1} in *NPH* and *NPT* ensembles, respectively, corresponding to a very viscous liquid.

We verify that the LDL phase is the liquid counterpart to amorphous silicon. To check this, we slowly heated a high quality amorphous model generated by a bond-switching technique described in [14] and relaxed with the SW potential, and compared with the LDL system. The amorphous phase is stable and does not crystallize after a long simulation (20 ns) at 1000 K. Its diffusivity increases rapidly at 1050 K, however, and it reaches a value very similar to that for the LDL at the same temperature, crystallizing within 12 ns (with 80 at.% of elementary blocks). This nucleation time is similar to that observed in the LDL obtained by cooling in the *NPT* and *NPH* ensembles (see figure 4). The degree of crystallization in figure 4 (top) after 20 ns seems to be closely related to the quality of the network in the initial state, as defined by its coordination. The amorphous model, with an initial coordination 4, crystallizes to 84%,

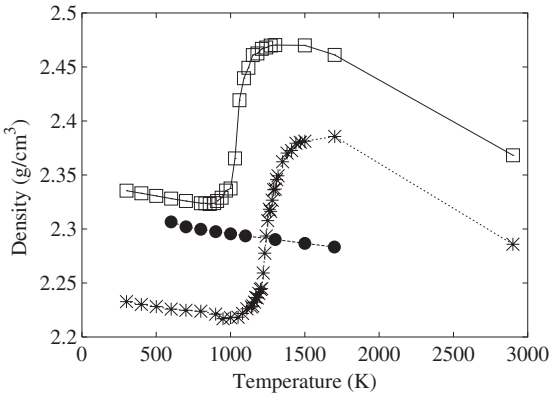

Figure 5. The density dependence of the temperature for liquid and crystalline silicon. We show the results for the crystal (•) and liquid at zero GPa (□) and −2 GPa (∗). At zero pressure, the supercooled liquid undergoes a first-order transition at around 1060 K. Curves are guides to the eyes.

while only 66 and 71% of atoms belong to basic block structures for the liquids cooled in the *NPT* and *NPH* ensembles, with average coordinations of 4.41 and 4.24 respectively.

Since the phase transition is buried deeply in the supercooled region, it is difficult to reverse the transition and go from LDL to HDL. Heated in steps from 1050 K, the LDL phase remains stable until it crystallizes at around 1150 K, showing considerable hysteresis. In order to reach HDL, it is necessary to bring the LDL system at once from 1050 to 1250 K, a feature already noted by Broughton and Li [15]. The HDL phase, in contrast, is stable against crystallization and does not show any significant density of elementary crystalline blocks even after 20 ns of simulation at a temperature as low as 1100 K.

3.1.2. Negative pressure. As discussed in the previous section, the LDL phase of the SW potential shows an average coordination of 4.24 at 1050 K, indicating the presence of a large fraction of mostly fivefold-coordinated atoms. This coordination is significantly higher than the experimental measurement indicates, which is an average coordination of 3.88 [26], and than the theoretically accepted value of 4.0 [13, 40, 14]. Such a discrepancy is largely due to the limits of the potential. As discussed in [13], for example, the SW potential systematically produces an overcoordinated amorphous phase; even very slow cooling fails to produce configurations near an average coordination of 4.0 [29].

Because of this discrepancy, it is important to test the stability of the LDL phase as the system is biased towards obtaining a higher quality amorphous phase. It is possible to favour the formation of a lower coordinated liquid by applying a negative pressure to the system or by changing the potential. In this section, we study the HDL to LDL change at a negative pressure of −2 GPa, near to the stability limit of the liquid; the effects of a potential change are studied in the next section.

To first order, the application of negative pressure simply shifts the phase diagram (figure 5), as the density maximum moves from 1300 to 1700 K and the liquid–liquid transition from 1060 to 1250 K, in agreement with the isochoric cooling curves as a function of density presented by Angell *et al* [7].

Similarly, the HDL to LDL transition remains at negative pressure. However, the system does not emit latent heat during the transition, and *NPH* simulations, with cooling steps of 10 K, closely follow the *NPT* curve (see figure 6). The HDL transforms, therefore, via a second-order

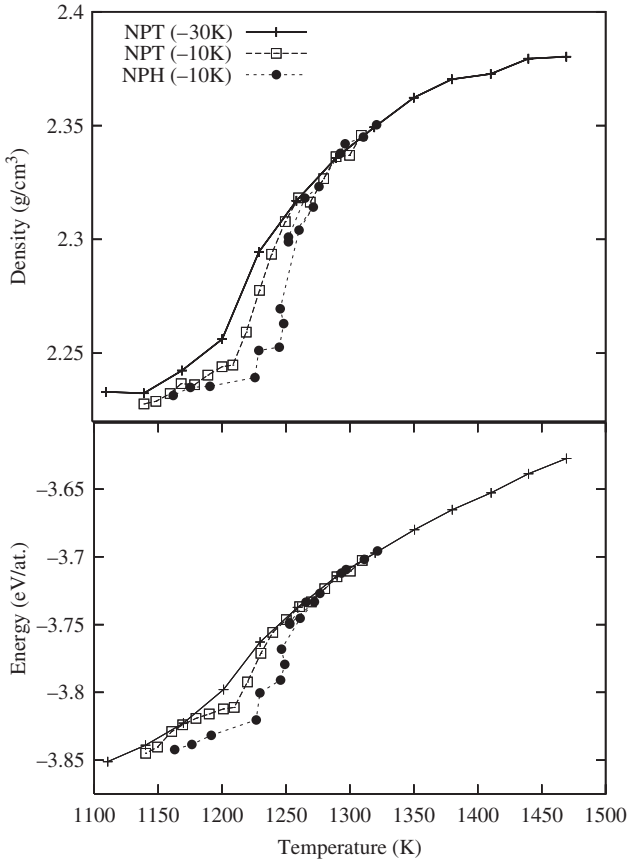

Figure 6. Mean density (top) and energy (bottom) as a function of temperature for a system maintained at a negative pressure of −2 GPa. The crosses (solid curve) show the results of an *NPT* simulation starting from a well-relaxed liquid configuration at 1500 K and then gradually lowering in steps of 30 K. The open squares (dashed curve) and the filled circles (dotted curve) correspond, respectively, to simulations in the *NPT* and *NPH* ensembles with an initial liquid configuration equilibrated at 1340 K where the temperature is lowered in steps of 10 K. Curves are guides to the eye.

phase transition into a lower density phase. During the transition, between 1270 and 1225 K, the system transforms into a tetravalent structure with the average coordination falling from 4.95 to 4.18 in *NPH* conditions and the proportion of atoms in crystalline structures increases from 5% to 30% (figure 7). At 1225 K, the diffusivity of the LDL is 1.6×10^{-7} cm^2 s^{-1}, and it is therefore still a liquid.

The theoretical model of Aptekar [9] locates the liquid–liquid transition at around 1500 K for Si at zero pressure and predicts a second critical point that terminates the first-order transition at −1.5 GPa in the supercooled liquid region. At −2 GPa, this model should therefore be below the critical point. Our picture is more complex, as there is now a second-order phase transition between the HDL and LDL, indicating that the critical point does not correspond to the end of a coexistence line.

3.1.3. Modified potential. High quality amorphous structures require a significant strengthening of the three-body term of the SW potential; an increase of 50% is necessary

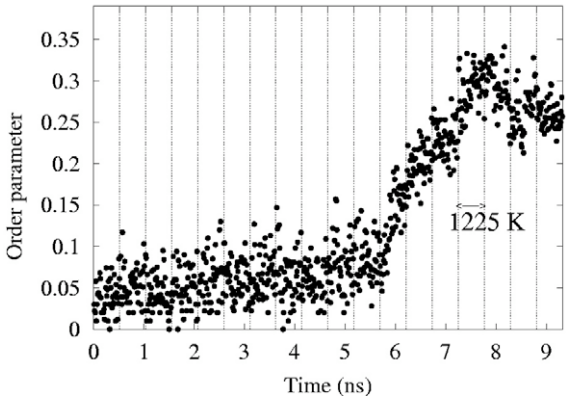

Figure 7. Evolution of the proportion of atoms in crystalline structures for the simulation in the *NPH* ensemble at a negative pressure of −2 GPa. Each section represents a time interval at a given enthalpy with the kinetic energy reduced by 5 K at the end of each interval. Each interval corresponds to a thermodynamic point in the density versus temperature figure (see figure 6). The double arrow indicates the time interval for which the average temperature is 1225 K.

to ensure a coordination of 4 in the amorphous phase for this potential [40, 28, 15]. This strong modification of the potential, however, completely changes the phase diagram of the system, removing the maximum in the density of the liquid phase and setting a lower density for the liquid as compared with the crystal. Although a 12.5% modification to the three-body term restores the temperature of density maximum in the liquid phase, the amorphous (or glassy) state reaches a lower density than the crystal. Thus, in order to preserve the main features of the SW phase diagram, we use much weaker modification, increasing the three-body term by 5%, in order to verify the universality of the liquid–liquid phase transition.

The transition from the high to low density phase has features similar to those for the original SW potential. In particular, a net release of latent heat confirms that the transition is first order. However, the small strengthening of the three-body term augments significantly the nucleation rate of Si and raises the transition temperature from 1060 to 1390 K (figure 9), indicating that the transition is qualitatively different. Indeed, the new phase, obtained following either the *NPT* or the *NPH* conditions, is already considerably crystalline at the transition: local order analysis shows that the *NPH* configuration at 1390 K and 2.28 g cm^{-3} occurring during the transition is crystallizing, with 55% of all atoms belonging to crystalline structures. The liquid–liquid transition is therefore totally hidden by the crystallization.

Because of the crystallization, the *NPH* and *NPT* simulations do not finish in the same thermodynamical state after the transition, contrarily to what is observed with the original SW potential: the *NPT* simulation shows a much more rapid crystallization than the *NPH* and, at 1290 K, more than 95% of all atoms are in a crystalline environment against 67% for the *NPH* simulation. This high degree of crystallinity can be seen directly in the RDF, as shown in figure 10: at 1390 K, only the *NPT* simulation shows a third-neighbour peak, while it is visible also in the *NPH* simulation at 1290 K.

4. Discussion and conclusion

The liquid–liquid transition in Si is difficult to observe because it should occur deep in the undercooled region of the phase diagram. It is not clear whether this part of the phase diagram can be reached experimentally, so we must rely on simulations to characterize this important phenomenon. Even with the fast cooling accessible to molecular dynamics investigation, the

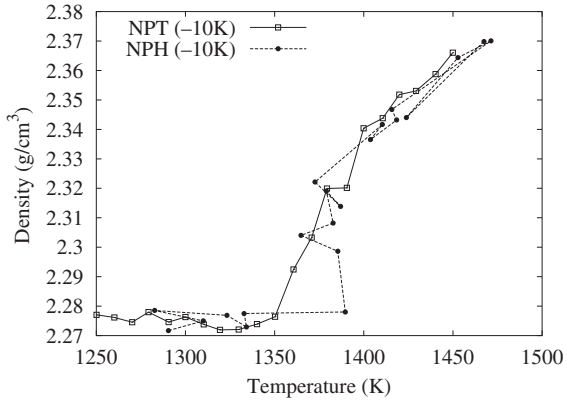

Figure 8. Density as a function of temperature with the modified SW potential ($\lambda = 1.05\lambda_0$). The open squares (solid curve) and the filled circles (dashed curve) show the result of simulation in the *NPT* and *NPH* ensembles, respectively, with cooling in steps of 10 K starting from an equilibrated l-Si configuration at 1460 K. Curves are guides to the eye.

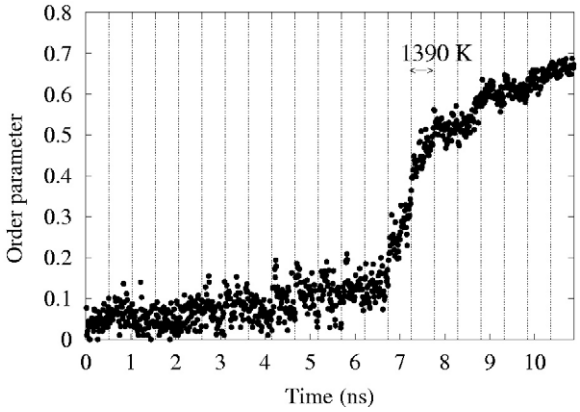

Figure 9. Evolution of the proportion of atoms in crystalline structures for a simulation in the *NPH* ensemble with the modified SW potential. Each section represents a time interval at a given enthalpy with the kinetic energy reduced by 5 K at the end of each interval. Each interval corresponds to a thermodynamic point in the density versus temperature figure (see figure 8). The double arrow indicates the time interval for which the average temperature is 1390 K.

temperature window for observing the LDL is very narrow and the viscosity increases rapidly as the LDL becomes glassy a-Si. This difficulty explains why the phase was only demonstrated recently for SW Si.

At zero pressure, Sastry and Angell [36] demonstrated the existence of a liquid–liquid phase transition in the SW Si. Moreover, we were able to verify that the amorphous phase, obtained via an independent method, does correspond to the LDL, as was suggested previously.

The question remains as to whether the LDL phase also exists in the real material. By moving around this thermodynamical point, it is possible to verify the stability of this result and whether or not this phase is likely to occur in Si.

As one of the main limitations of the SW potential is that it cannot be used to properly describe the structure of the amorphous phase, corresponding to the glassy phase of LDL,

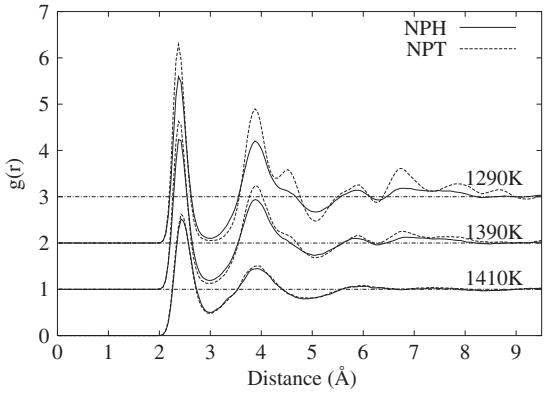

Figure 10. The radial distribution function of the modified SW potential near the transition temperature in the *NPT* and *NPH* ensembles. The RDFs are measured at different temperatures: 1290 K (top), 1390 (middle) and 1410 K (bottom).

we look at the impact of getting better coordinated a-Si on the phase diagram by applying a negative pressure and slightly changing the potential.

Following the analysis of Aptekar, a critical point should exist at the end of the coexistence line below −1.5 GPa [9]. We find instead that the order of the liquid–liquid transition changes from first to second, with an absence of heat release during the transition. The relative change in structure from HDL to LDL is very similar to that obtained at zero pressure, however, and the average coordination is closer to 4.0. Nevertheless, the LDL seems to be even more unstable under crystallization than at zero pressure.

It is also possible to favour a lower coordination in the amorphous phase by increasing the strength of the three-body force of the SW potential. To keep the same overall phase diagram, we modify this term only very slightly, increasing it by only 5%. The impact of this modification is surprisingly important: the first-order transition moves from 1060 to 1390 K and changes in character, crystallization occurs almost immediately and there is no trace of a low density liquid. The temperature shift is much larger than the change in melting temperature, which is about 20 K, suggesting that the transition seen with the strengthened potential is the standard crystallization transition in the undercooled phase. The liquid–liquid transition, if present, is therefore not easily reachable even on the MD timescale. This is particularly clear using a topological order parameter which identifies the degree of crystallinity with much more precision than averaged structural quantities such as the structure factor and the RDF.

The SW potential fails to describe the amorphous state of silicon and small changes in the potential are shown to modify the behaviour of the phase transition; hence an enhanced version of this potential for the low temperature phases of silicon would yield better insight into phenomena far from the melting point. While the results of Sastry and Angell provided the first clear demonstration of the existence of a liquid–liquid first-order transition in SW Si [36], our results suggest that the existence and the nature of the liquid–liquid phase transition in real Si must be confirmed through further simulations with a wider set of potentials and, if possible, through experiment.

Acknowledgments

This work was funded in part by NSERC, NATEQ and the Canada Research Chair Program. NM is a Cottrell Scholar of the Research Corporation. Most of the simulations were run on the

computers of the Réseau québécois de calcul de haute performance (RQCHP), whose support is gratefully acknowledged.

References

[1] Aasland S and McMillan P 1994 *Nature* **369** 633
[2] Allen M and Tildesley D 1987 *Computer Simulation of Liquids* (Oxford: Oxford University Press)
[3] Andersen H 1980 *J. Chem. Phys.* **72** 2384
[4] Angell C and Borick S 1999 *J. Phys.: Condens. Matter* **11** 8163
[5] Angell C and Borick S 2000 *Phys. Chem. Chem. Phys.* **2** 1559
[6] Angell C and Borick S 2002 *New Kids of Phase Transition: Transformations in Disordered Substances* ed V V Brazhkin *et al* (Dordrecht: Kluwer–Academic) pp 29–46
[7] Angell C, Borick S and Grabow M 1996 *J. Non-Cryst. Solids* **205–207** 463
[8] Ansell S, Krishnan S, Felten J and Price D 1998 *J. Phys.: Condens. Matter* **10** L73
[9] Aptekar L 1979 *Sov. Phys.—Dokl.* **24** 993
[10] Ashcroft N W and Mermin N 1976 *Solid State Physics* Thomson Learning
[11] Baeri P, Foti G, Poate J and Cullis A 1980 *Phys. Rev. Lett.* **45** 2036
[12] Balamane H, Halicioglu T and Tiller W 1992 *Phys. Rev.* B **46** 2250
[13] Barkema G and Mousseau N 1996 *Phys. Rev. Lett.* **77** 4358
[14] Barkema G and Mousseau N 2000 *Phys. Rev.* B **62** 4985
[15] Broughton J and Li X 1987 *Phys. Rev.* B **35** 9120
[16] Brown D and Clarke J 1984 *Mol. Phys.* **51** 1243
[17] Cook S J and Clancy P 1993 *Phys. Rev.* B **47** 7686
[18] Donovan E, Spaepen F, Turnbull D, Poate J and Jacobson D 1985 *J. Appl. Phys.* **57** 1795
[19] Durandurdu M and Drabold D 2001 *Phys. Rev.* B **64** 14101
[20] Egry I 1999 *J. Non-Cryst. Solids* **250–252** 63
[21] Evans D and Morris G 1984 *Comput. Phys. Rep.* **1** 297
[22] Funamori N and Tsuji K 2002 *Phys. Rev. Lett.* **88** 255508
[23] Haile J and Graben H 1980 *J. Chem. Phys.* **73** 2412
[24] Hoover W 1983 *Annu. Rev. Phys. Chem.* **34** 103
[25] Katayama Y, Mizutani T, Utsumi W, Shimomura O, Yamakata M and Funakoshi K 2000 *Nature* **403** 170
[26] Laaziri K, Kycia S, Roorda S, Chicoine M, Robertson J, Wang J and Moss S 1999 *Phys. Rev. Lett.* **82** 3460
[27] Landman U, Luedtke W, Barnett R, Cleveland C, Ribarsky M, Arnold E, Ramesh S, Baumgart H, Martinez A and Khan B 1986 *Phys. Rev. Lett.* **56** 155
[28] Luedtke W and Landman U 1988 *Phys. Rev.* B **37** 4656
[29] Luedtke W and Landman U 1989 *Phys. Rev.* B **40** 1164
[30] Mishima O and Stanley H E 1998 *Nature* **396** 329
[31] Mishima O and Stanley H E 1998 *Nature* **392** 164
[32] Nakhmanson S and Mousseau N 2002 *J. Phys.: Condens. Matter* **14** 6627
Beaucage P and Mousseau N 2005 *Phys. Rev.* B **71** 094102
[33] Ohtaka O, Arima H, Fukui H, Utsumi W, Katayama Y and Yoshiasa A 2004 *Phys. Rev. Lett.* **92** 155506
[34] Poole P, Grande T, Angell C and McMillan P 1997 *Science* **275** 322
[35] Saika-Voivod I, Poole P and Sciortino F 2001 *Nature* **412** 514
[36] Sastry S and Angell C 2003 *Nat. Mater.* **2** 739
[37] Sciortino F, Nave E L and Tartaglia P 2003 *Phys. Rev. Lett.* **91** 155701
[38] Stillinger F and Weber T A 1985 *Phys. Rev.* B **31** 5262
[39] Thompson M, Galvin G, Mayer J, Peercy P, Poate J, Jacobson D, Cullis A and Chew N 1984 *Phys. Rev. Lett.* **52** 2360
[40] Vink R, Barkema G, van der Weg W and Mousseau N 2001 *J. Non-Cryst. Solids* **282** 248
[41] Waseda Y 1980 *The Structure of Non-Crystalline Materials; Liquid and Amorphous Solids* (New York: McGraw-Hill)
[42] Waseda Y, Shinoda K, Sugiyama K, Takeda S, Terashima K and Toguri J M 1995 *Japan. J. Appl. Phys.* **34** 4124